Design of a two-wheel tractor operated onion harvester

Getu Tesfaye[1*], Amana Wako[2]

*(1. Department of Agricultural Mechanization, Alage ATVET College, Alage, 77, Ethiopia;
2. Department of Mechanical Engineering, Adama Science and Technology University, Adama, 1888, Ethiopia)*

Abstract: Onion is a root crop that had been harvested manually in Ethiopia which was tedious, consumes time, labor-intensive, and costly operation. The main objective of this study was to design, fabricate, and perform the evaluation of a two-wheel tractor operated onion harvester to alleviate the above-stated problems. A two-wheel tractor operated onion harvester has not designed specifically in Ethiopia and the designed machines should have cutting disc and collector for effective harvesting operation. The physical properties of onion and soil relevant to the design of the digger were studied and each component of the machine was designed accordingly. The design of the harvester was based on the use of locally available materials to reduce costs. A prototype of the harvester was constructed and tested in the field to evaluate its performance. The performance of the harvester was evaluated based on its efficiency, productivity, and cost-effectiveness. The maximum and minimum digging efficiency of the machine was 97.03% at 1.39 km h^{-1} forward speed and 10 cm depth of operation and 84.60% at 4.15 km h^{-1} forward speed and 5 cm depth of operation respectively. The maximum mean damage percentage, missing percentage, drawbar pull, fuel consumption, wheel slip, field efficiency, and field capacity were 4.56%, 11.36%, 2935.4 N, 15.51 l ha^{-1}, 20.82%, 90.84% and 0.157 ha h^{-1} respectively. Based on the results, the machine was found to be acceptable for use by small-scale farmers.

Keywords: Design, fabrication, evaluation, forward speed, depth of operation, onion tuber

Citation: Tesfaye, G., and A. Wako. 2025. Design of a two-wheel tractor operated onion harvester. Agricultural Engineering International: CIGR Journal, 27(4):80-101.

1 Introduction

Onion (Allium Cepa) is a genus of vegetable that thought to have originated in Southwest Asia and have since spread throughout the world (Brewster, 2008; Kitila et al., 2022). The most active onion producers were China, India, the United States, Turkey, Japan, Spain, Brazil, Poland and Egypt (Elyazaji, 2024). Ethiopia was one of the top three onion producing countries in Africa after Egypt and South Africa, producing 2.7% of world production between 2000 and 2011 (FAOSTAT, 2019). Onion is an important and profitable crop grown by both small farmers and large companies in Ethiopia for both local consumption and export (Aklilu, 1994; Etana et al., 2019). It was the second most productive vegetable crop after tomatoes, grown mainly in the upper Awash and Lake Ziway areas of the central rift valley of the country (Hunde, 2017; Etana et al., 2019). During 2017-2018, Oromia region alone produced 13,669.5 tons of onions per hectare, totaling 1,033,485.45 tons of onions with an average yield of 7.56 tons per hectare (Fikre, 2021).

Harvesting is an important process in onion cultivation. Manual harvesting is the most common practice in developing countries, involving digging onions from the ground with a hand shovel, which can be time- and labor-intensive. Manual harvesting is not only slow, but also involves a lot of work and losses. The study also showed that manual labor can require 403 man-hours per hectare, compared to 390 man-

Received date: 2024-02-09 **Accepted date:** 2025-07-10

***Corresponding author: Getu Tesfaye.** Department of Agricultural Mechanization, Alage ATVET College, Alage, 77, Ethiopia. Email: keraj2016@gmail.com.

hours for semi-mechanical harvesting operations (Laryushin and Laryushin, 2009). This is labor intensive and labor intensive. Traditional harvesting methods have significant disadvantages, including high labor costs (Anon, 2018). Mechanical harvesting is an option used by farmers in economically developed countries, particularly on large farms. Machines are generally used to harvest onions quickly and efficiently with lower labor. The harvester is used as an automated process that begins with loosening the soil and ends with removing the onion and its leaves from the soil (Erokhin et al., 2022).

The land of smallholder farmers in Ethiopia is often small, hilly and fragmented. A rototiller is a type of tractor specifically designed for use on small to medium-sized farms, called an electric rototiller, rototiller, hand tractor or garden tractor, and is used primarily for rotary tillage and other tasks (Kebede and Getnet, 2017). The cleaned onion bulbs are then removed into the collector. As the 2WT progresses; the harvester finally lays the onion bulbs into narrow strips, making it easier to harvest the onions. This research was unique in that previously developed tractor-driven two-wheel onion harvesters did not have a cutting disc, a harvester, or a specially designed tractor-driven two-wheel onion harvester from Ethiopia.

Therefore, this study was aimed to design, develop, and evaluate the performance of a 2WT-operated onion harvester that is affordable for Ethiopia's small-scale farmers and the designed harvester would save time and labor as well as reduce physical effort for farmers during harvesting.

2 Materials and method

2.1 Soil properties

The experiment was conducted at Kulumsa Agricultural Research Center during 2022 main rainy season. Kulumsa Agricultural Research Center (KARC) is located at 8°00‟ to 8 o 02‟N latitude and 39°07’’ to 39°1’’E longitude with an altitude of 2200 m.a.s.l. The annual minimum and maximum temperatures of 10°C and 22°C and the soil texture is luvisol soils in Tiyo district, Arsi administrative zone.

2.1.1 Shear strength

According to ASTM (2002), soil shear strength is contributed by cohesion and angle of internal friction.

$$\tau = \frac{6}{7}\left(\frac{T}{\pi D^3}\right) \quad (1)$$

Where:

τ= Shear strength (N/m²)

T= torque (N/ m)

D= diameter (m)

2.1.2 Penetration resistance

Soil penetration resistance is a crucial factor in the mechanized harvesting of onions. High soil penetration resistance can hinder the efficiency of harvesting machines, leading to increased energy consumption and potential damage to the crop. Recent studies have focused on optimizing the design and operation of onion harvesters to address this challenge. By optimizing soil penetration resistance and other mechanical properties, these studies contribute to the development of more efficient and effective onion harvesting machines, ultimately improving productivity and reducing labor costs.

2.2 Onion bulb properties

2.2.1 Size

Each of the 100 bulbs' thickness, polar diameter, and equatorial diameter were determined using a caliper with a resolution of 0.01 mm. The Arithmetic mean was calculated using the equation described by Mohsenin (1986).

$$Ad = \frac{(D_e + D_p + t)}{3} \quad (2)$$

Where:

Ad= arithmetic mean diameter, cm

D_e = equatorial diameter, cm

D_p = polar diameter, cm

t= thickness, cm

2.2.2 Moisture content

A 50 g sample was weighed, placed in an empty moisture box, and its combined weight was recorded. For 24 hours, the moisture box was placed in oven dry at 105°C ± 2°C. The formula below can be used to calculate the onion's moisture content.

$$Mc = \frac{M2-M3}{M2-M1} \times 100 \quad (3)$$

Where:

M_c=moisture content, % (W.b) ;

M_1=weight of moisture box, g;

M_2= weight of moisture box + tuber before drying, g;

M_3= weight of moisture box + onion tuber after drying, g.

2.2.3 Coefficient of static friction

The galvanized sheet, mild steel, aluminum sheet, and plywood were used to determine the onion bulb coefficient of static friction (μ). The slope was gradually raised while the onion was kept on a horizontally level surface. The experiment was repeated three times, and the mean inclination angle was calculated. The coefficient of static friction was:

$$\mu = tan\,\alpha \quad (4)$$

Where:

α= angle of inclination (^{0})

Determining the coefficient of static friction involves a few key steps. Here's a general procedure:

(1) Set up the equipment: It needs a flat surface, a block of known mass, a force sensor or spring scale, and a way to measure the normal force (usually the weight of the block).

(2) Measure the normal force: Calculate the normal force (Nf) by multiplying the mass of the block (m) by the acceleration due to gravity (g = 9.81 m s^{-2}). So, $N = m \times g$.

Where:

Nf=Normal force (N)

m=mass (Kg)

(3) Apply a horizontal force: Gradually apply a horizontal force to the block using the force sensor or spring scale until the block just starts to move. This force is the maximum static friction force (Fs).

(4) Record the maximum static friction force: Note the value of the force at the moment the block starts to move. This is the maximum static friction force.

(5) Calculate the coefficient of static friction

2.2.4. Coefficient of friction

The coefficient of friction is an important parameter in the design and operation of onion harvesters. It affects the efficiency of soil and onion separation during harvesting. Recent research has highlighted the importance of selecting appropriate materials for the construction of harvester components to minimize friction and reduce damage to the onions. For instance, the static coefficient of friction for onion seeds varies depending on the surface material, with values ranging from 0.2878 to 0.63813. Using materials with lower coefficients of friction can help improve the efficiency of the harvesting process and reduce mechanical damage to the onions.

2.2.5 Hardness

The hardness of an onion bulb is a key quality attribute that affects its handling, storage, and processing. Hardness is typically measured using a durometer, which assesses the resistance of the onion bulb to deformation. This method is non-destructive and provides reliable results that are closely correlated with those obtained from tensile testing machines.

Recent studies have shown that the hardness of onion bulbs can vary significantly based on factors such as variety, growing conditions, and storage methods. For instance, onions stored in forced ventilated and natural ventilated conditions tend to have higher hardness values compared to those stored in traditional systems (Hatem et al., 2014). This is because controlled storage conditions help maintain the structural integrity of the onion bulbs, reducing the likelihood of softening and spoilage.

2.3 Power required for soil cutting

Thewidth of digger blade was an important factor, as it would cover all plant rows in a bed without damaging standing crop. Therefore, it was decided on the basis of the width of the bed that the mutated stem crop was grown in rows. Onion digger having maximum depth and width of 10 cm and 36 cm respectively that was depth with width ratio of 0.208 which is less than 0.5 called as wide blade (Khura, 2008). The soil cutting force of the blade was calculated using Equation 5.

$$Fs = \left(\gamma d^2 N_\gamma + qdN_q + CdN_c + C_a dN_{ca}\right)w \quad (5)$$

Where:

γ = unit weight of soil, kg m^{-3}

C = apparent cohesion, kN m^{-2}

Ca = soil-interface adhesion, kN m^{-2}

d = depth of cutting, m

w = width of cutting, m

q = surcharge pressure on soil, kN m^{-2}

F_s = soil resistance force (kN)

N_γ = soil friction cutting coefficient

N_q = soil overburden cutting coefficient

N_c = soil cohesion cutting coefficient

N_{ca} = soil adhesion cutting coefficient

$N\gamma$, Nc, Nca, Nq are dimensionless Reece factors, which states the shape of soil-failure surface.

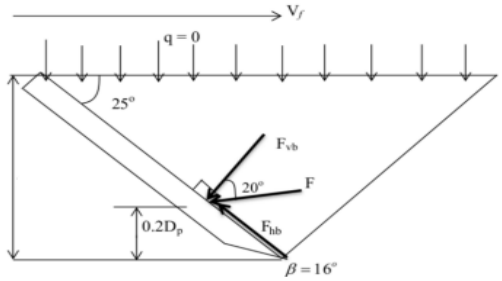

Figure 1 Forces applied on digging blade

Based on suggestions and presumptions made by various works of literature during the design and evaluation of tillage implements and root crop harvesters, the estimated soil cutting force (Fs) of the onion harvester was developed. Surcharge (q) and machine adhesion (Ca) of soil utilized by various researchers can be regarded as insignificant. Equation (5) can therefore be simplified to Equation (6):

$$Fs = \left(\gamma d^2 N_\gamma + CdN_c\right) \times w \quad (6)$$

The relationship between the N factors and the rake angle at different angle of internal friction for a blade with perfectly smooth (δ=0) and perfectly rough ($\delta = \Phi$) (Hettiaratchi et al., 1966). The values of N factors for intermediate degree of roughness of the interface can be interpolated using the following equation (McKyes, 1989):

$$N = No\left(\frac{N\emptyset}{No}\right)^{\frac{\delta}{\emptyset}} \quad (7)$$

Where:

N_δ = the required value of the appropriate N factors like as N_γ or N_c;

N_δ = 0;

$N_\delta = \Phi$ are the corresponding value of the N-factor at δ = 0;

$\delta = \Phi$, respectively obtained from appropriate chart.

Based on the assumptions made above, values of optimum parameters were listed below for the determination of soil passive resistance (Budhale et al., 2019).

γ = 1450 kg m^{-3}, C= 30.18 KN m^{-1} $\Phi = \delta$ =20°, α = 25° and d = 0.1 m

Value of N-factor was selected as follows:

N_γ = 1.65 when δ = 0

N_γ = 1.83 when $\delta = \Phi$

N_c = 1.72 when δ = 0

N_c = 1.68 when δ = 20

Now substituting the values of N_γ and N_c determined, the passive resistance (F_s) is given as:

$$Fs = \left(1450 \times 9.81 \times \left(0.1\text{m}\right)^2 \times 1.83 + 30.18\frac{\text{N}}{\text{m}^3} \times 1000 \times 0.1\text{m} \times 1.68\right) \times 0.36\text{m} = \left(260.308\ \text{Nm} + 5070.24\frac{\text{N}}{\text{m}}\right) \times 0.36\text{m} = 1919\ \text{N}$$

The passive resistance force (Fs), according to Khura (2008), is acting at an angle of friction (δ) with normal and perpendicular to the contact of a blade. Hence, the component parallel to the blade face (F_h) was: $Fh = Fs \sin\delta$

$$\text{Fh} = 1919\ \text{N} \sin 20^o = 656.34\ \text{N}$$

Component perpendicular to the blade face (F_v) was given as:

$$\text{Fv} = \text{Fs}\cos\delta \quad (8)$$

$$\text{Fv} = 1919\text{N}\cos 20^o = 1803.27\text{N}$$

Power required for soil cutting (P_{sc}) was:

$$\text{Psc} = \text{Fs} \times \text{V} \quad (9)$$

Where:

F_s = soil resistance force, (N)

V = operating speed (m s^{-1}), let's take V=3.5 Km hr^{-1} = 0.972 m s^{-1}

$$\text{Psc} = 1919\text{N} \times \frac{0.972\text{m}}{\text{s}} = 1865.27\text{w}$$

2.4 Design and construction of soil cutting blade

The front end of the conveyor has a trapezoidal-shaped blade with a significant width. While Fv is the vertical component which would result in a bending moment and Fh is the horizontal component which would place direct stress on the blade. It was assumed that average soil resistance of the blade acts at a distance of $0.2z_1$, measured from the cutting edge (Bernacki et al., 1972).

The blade is supported on the shank at a distance 200 mm from the cutting edge. Therefore, the distance between the center of resistance and point of support (Dr) could be determined by:

$$Dr = 100mm - 0.2 \times 100\ mm = 80mm$$

Length of blade from blade support to center of resistance (y):

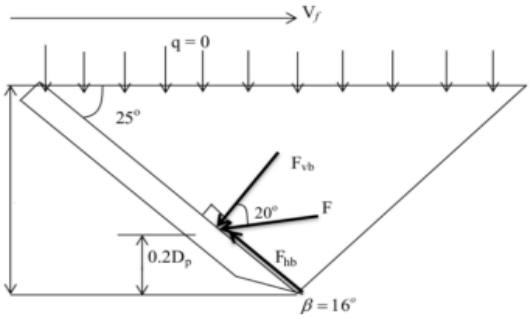

Figure 2 Soil reactions acting on a blade (Khura, 2008)

Therefore, the bending moment (M) due to Fv would be:

$$M = Fv \times y \quad (10)$$

$$M = 1803.27N \times 189.3mm = 341{,}359Nmm$$

Bending stress on the blade (σb) is:

$$\sigma b = \frac{M}{\frac{1}{6}bt^2} \quad (11)$$

$$\sigma b = \frac{341{,}359Nmm}{\frac{1}{6}\times 720mm\times t^2} = \frac{2844.66N}{t^2}$$

Direct stress (σ_d) due to F_h was:

$$\sigma d = \frac{Fh}{b\times t} \quad (12)$$

$$\sigma d = \frac{656.33N}{720mm\times t} = \frac{\frac{0.91N}{mm}}{t}$$

Total stress (σ) could be determined as follows:

$$\sigma t = \sigma b + \sigma d \quad (13)$$

$$\sigma t = \frac{2844.66N}{t^2} + \frac{\frac{0.91N}{mm}}{t}$$

By taking factor of safety 3 for agricultural machines (Sharma and Mukesha, 2010) and yield stress of 294.74 MPa of AISI 1020 mild/low carbon and by equating the total stress, the thickness of blade (t) was determined as:

$$\sigma y = \left(\frac{2844.66N}{t^2} + \frac{\frac{0.91N}{mm}}{t}\right) \times fos \quad (14)$$

$$294.74Mpa = \left(\frac{2844.66N}{t^2} + \frac{\frac{0.91N}{mm}}{t}\right) \times 3$$

$$t \approx 6\ mm$$

The width of blade was calculated as effective zone of triangular V-shaped blade was (Sharma and Mukesha, 2010):

$$Zf = w + 2d\tan\emptyset \quad (15)$$

Therefore, width of onion digger blade was computed as:

$$50cm = w + 2 \times 10cm \tan 35^o$$

$$w \approx 36\ cm$$

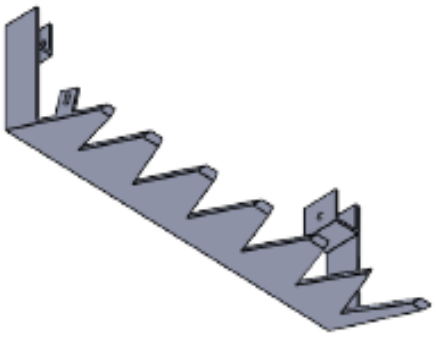

Figure 3 Digging blade

The solid work force analysis of the model is carried out to optimize the design by analyzing the reaction of blade under the loading conditions. As per the design calculations, the thickness of the blade is 6 mm and it is tested under the draft forces acting on the blade. The boundary condition is considered as the zero displacements of the side end of the blade at top corners, which will be joined to the conveying system. The forces applied on each tip of the blade and the resulting total deformation and equivalent stress has been verified and ascertained to be safe. Figure 3 shows that the plot type being analyzed was static displacement which likely refers to the displacement of an object or structure under a static load. The deformation scale is given as 7.01157, which could refer to the amount of deformation or strain being analyzed in the study.

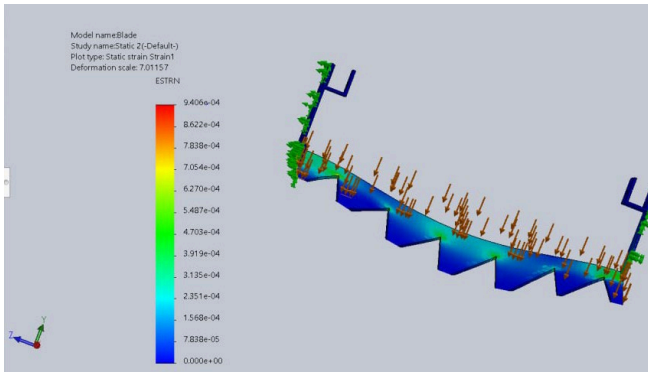

Figure 4 Solid work force analysis

2.5 Design of conveyor and separation unit

The separation unit was placed directly behind the blade to separate the soil from the crop. The separation unit consists of stainless-steel plates with a round shape that were arranged along the line of travel of the onion digger. The conveyor is mounted at the rear end of the digger blade and consists of two shafts with ball bearings fixed apart at the center distance of 680mm. Four sprockets of 9.5 cm diameter with two chains combination were mounted on the conveyor shafts

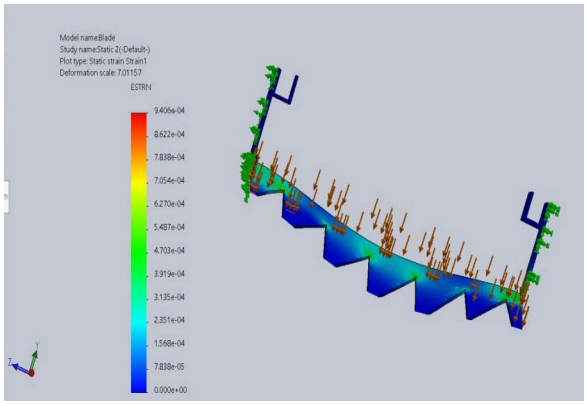

Figure 5 Force analysis on digging blade

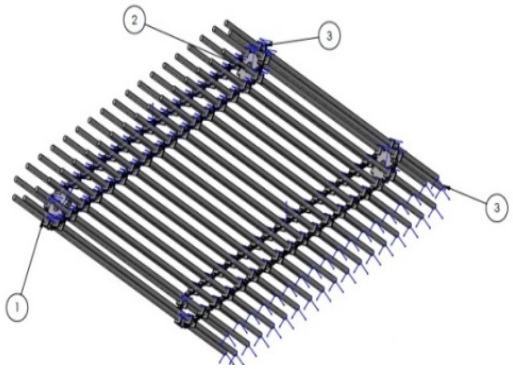

Figure 6 Conveyor and separation unit

Note: 1: Conveyor chain, 2: Conveyor sprocket and 3: Rod bar

2.6 Selection of conveyor chain and sprocket

Dessye (2021) studied a conveyor chain drive with two chain and sprocket wheel combinations on opposite sides of the conveyor web. The chain drive was operating at 3.14 m s^{-1} which was necessary in order to reach the desired speed of 1.5 m s^{-1} and have a power output of 983.97 W. In order to calculate the overall service factor a few different factors were taken into account. The load factor takes into consideration the amount of variable load, with a medium shock factor, which was set to K_1=1.25. There was also a lubrication factor for periodic lubrication, set to K_2= 0.85, and a rating factor for 8-hours of operation per day, set to K_3=1.

$$Ks = K1 \times K2 \times K3 \quad (16)$$

$$Ks = 1.25 \times 0.85 \times 1 = 1.875$$

$$Pd = Pc \times Ks \quad (17)$$

$$Pd = 528.5w \times 1.875 = 990.94w$$

The pitch circle diameter of the conveyor sprocket was:

$$V = \frac{\pi DN}{60} \quad (18)$$

$$1.5\frac{m}{s} = \frac{\pi \times D \times \frac{3.14m}{s}}{60} = D = 9.5\ cm$$

Load on the chain (W) could be (Khurmi and Gupta, 2005):

$$W = \frac{Pd}{Vc} \quad (19)$$

$$W = \frac{990.94\ w}{1.5\frac{m}{s}} = 660.62\ N$$

Factor of safety (fos) was calculated using the following equation:

$$fos = \frac{Wb}{W} \quad (20)$$

$$fos = \frac{28900N}{1229.96N} = 23.5$$

Center distance of chain and sprocket is center to center distance of conveyor was 68 m. Average velocity of the chain was given by the following equation:

$$T = \frac{60 \times Vc}{P \times N} \quad (21)$$

Where:

D = Pitch diameter of the sprocket, m

p = Pitch of the chain in meters, m

T = Number of teeth

$$T = \frac{60 \times \frac{1.5m}{s}}{0.01905mm \times \frac{3.14m}{s}} = 15$$

The required number of teeth on the large sprocket

for power transmission was:

$$V.R = \frac{N1}{N2} = \frac{T2}{T1} \quad (22)$$

$$T2 = 13 \times \frac{\frac{7.55m}{s}}{\frac{3.14m}{s}} = 15.6 \approx 16$$

$$D1 = \frac{P}{\sin\left(\frac{180^o}{T1}\right)} \quad (23)$$

$$D1 = \frac{15.875mm}{\sin\left(\frac{180^o}{13}\right)} = 66mm$$

Pitch diameters of the driven sprocket also:

$$D2 = \frac{P}{\sin\left(\frac{180^o}{T2}\right)} \quad (24)$$

$$D2 = \frac{15.875mm}{\sin\left(\frac{180^o}{16}\right)} = 81.4mm$$

$$K = \frac{T1+T2}{2} + \frac{2x}{p} + \left(\frac{T2-T1}{2\pi}\right)^2 \quad (25)$$

$$K = \frac{13+16}{2} + \frac{2\times40}{15.875mm} + \left(\frac{16-13}{2\pi}\right)^2 = 95$$

$$L = K \times p \quad (26)$$

$$L = 95 \times 15.875mm = 1492.25mm$$

The total load on driving side of chain is the sum of tangential driving force (F_t), centrifugal tension on chain (F_c) and the tension due to sagging (F_s) (Khurmi and Gupta, 2005).

Hence,

$$Ft = \frac{P}{V} \quad (27)$$

$$Ft = \frac{983.97w}{\frac{1.246m}{s}} = 789.7N$$

$$Fc = mv^2 \quad (28)$$

$$Fc = \frac{1.2kg}{m} \times \left(\frac{1.246m}{s}\right)^2 = 1.863N$$

$$Fs = Kmgx = 4 \times \frac{1.2kg}{m} \times \frac{9.81m}{s^2} \times 0.680m = 29.67N$$

The total tension load on driving of chain (T):

$$T = Fc + Ft + Fs \quad (29)$$

$$T = 1.863N + 789.7N + 29.67N = 821.23N$$

Power required for driving (P_r) was:

$$Pr = T \times V \quad (30)$$

$$Pr = 821.23N \times \frac{1.246m}{s} = 1038.04w$$

The conveyor power (Pc) transmitted by thus chain and sprocket was 983.97 W at input speed of 360.1 rpm and output speed (conveyor rpm) of 3.14 m s^{-1}. A roller chain, minimum number of teeth on the driver sprocket (T_1) for a velocity ratio of 1.2 should be 13. Speed and pitch diameter of conveyor sprocket (D) is 3.14 m s^{-1} and 81.4 mm respectively. The driver sprocket was fixed at output shaft with rpm (N_o) and pitch diameter (D_o) is 7.55 m s^{-1} and 66.1 mm respectively. The Transmission ratio between input and output shaft could be:

$$\frac{Nm}{No} = \frac{Do}{Di} \quad (31)$$

Where:

D_o = pitch diameter of driven gear at output shaft, cm;

D_i = pitch diameter of driver gear at input shaft, cm;

$$\frac{\frac{29.66m}{s}}{\frac{7.55m}{s}} = \frac{Do}{Di} = 2.62$$

Distance from the center of the driving gear to the center of the driven gear (C_d) is the sum of the pitch radii of two gears in meshing (Mott, 2004):

$$Cd = \frac{(Do + Di)}{2} \quad (32)$$

Space available between output and input shaft (C_d) was 17.25 cm. Hence,

$17.25\ cm = \frac{(D_i + 2.3D_i)}{2}$, $D_i = 10.5$ cm,

$D_o = 24$ cm

The pitch diameter and number of teeth of the driving and driven gear were 10.5 cm, 24 cm, 30, and 70, respectively. This means that the driving gear had 10.5 cm in diameter and 30 teeth, and the driven gear had 24 cm in diameter and 70 teeth. The material used for the gears is called through-hardened steels (AISI 1020), which is a type of steel known for its durability, availability, and cost-effectiveness. The transmitted force, or F_t, and normal force, or F_n, on the gears has determined as below.

$$Ft = \frac{2To}{D} \quad (33)$$

$$Ft = \frac{2 \times 132.75Nm}{0.24m} = 1106.27N$$

$$Fn = Ft\tan\theta \quad (34)$$

$$Fn = 1106.27N \times \tan20^o = 402.65N$$

The power was transmitted between the shafts

using chain and sprocket mechanism that inclined to 20° to horizontal.

2.7 Design of conveyor rod

The length of chain conveyor L_c

$$K = \frac{T1+T2}{2} + \frac{2x}{p} + \left(\frac{T1-T2}{2\pi}\right)^2 \quad (35)$$

$$K = \frac{16+16}{2} + \frac{2\times 68cm}{1.905cm} + \left(\frac{16-16}{2\pi}\right)^2 = 103.39$$

$$Lc = 97.1 \times p = 103.39 \times 1.905cm = 196.95cm$$

Load applied on each conveyor rod (W_r) at a time was:

$$Wr = \frac{2(Qs)g}{nr} \quad (36)$$

$$Wr = \frac{2\times 88.26kg\times\frac{9.81m}{s^2}}{53} = 32.67N$$

Maximum bending Moment (M_{br}) at each conveyor rod is:

$$Mbr = \frac{Wr\times L}{2} \quad (37)$$

Where:

L= length of conveyor rod, mm

W_r = load acting on each conveyor rode, N

$$Mbr = \frac{32.67N \times 750mm}{2} = 1251.25mm$$

Maximum bending stress (σ_b) was:

$$\sigma b = \frac{32Mbr}{\pi d^3} \times fos \quad (38)$$

$$\sigma b = \frac{294.74N}{mm^2} = \frac{32 \times 1251.25Nmm}{\pi d^3} \times 3$$

$$d = 10.83mm \approx 12mm$$

Diameter of conveyor rod and minimum tuber diameter (D_{min}) was taken 12 mm and 25 mm respectively.

Spacing (S) between rods was using Equation (39):

Where:

S= space between conveyor rods, cm

Lc= total length of conveyor chain, cm

nr= number of conveyor rods

Dr=diameter of rod, cm

D_{min}=minimum onion tuber diameter (2.5 cm)

$$S = \frac{Lcs}{nr} - Dr \leq Dmin \quad (39)$$

Spacing between rods was:

$$S== \frac{197cm}{nr} - 1.2cm \leq 2.5cm, nr \geq 53rod$$

2.8 Design and analysis of output shaft

The output shaft is a uniform-diameter metal piece with a circular cross-section and small indentations called keyways which was used to transfer power from the input shaft to another component, like a spur gear. This component is then able to drive things like conveyor systems which might be exposed to a combination of both torsional (twisting) and bending forces. Figure 7 shows the design of the output shaft, which includes a driven gear, chain, driver sprocket, and bearings. The power (Kw) required to drive the output shaft is calculated by multiplying the torque developed by the speed of the shaft. In addition, the output shaft is subject to horizontal.

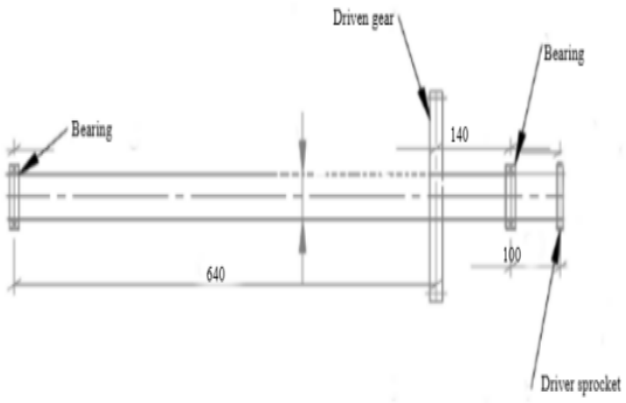

Figure 7 Output shaft with a driven gear, chain, driver sprocket and bearings

The power driven by output shaft (P_o) was:

$P_o = P_c = 807.13$ W

Hence, torque developed by output shaft (T_o) at N_o=360.1 rpm was:

$$To = \frac{Po\times 60}{2\pi\times No} \quad (40)$$

Where:

P = power require to drive, kW

N_o = Speed of the shaft, rpm

F = force required to drive the machine, N

r = radius of shaft, m

$$To = \frac{807.13w \times 30}{2\pi \times 0.015 \times \frac{7.55m}{s}} = 1427.64\ Nm$$

Bending and twisting moment occur on shaft as a result of applied loads, belt and chain tensions. Out shaft was subjected to both horizontal and vertical load acting on the shaft.

Horizontal forces acting on output shaft was:

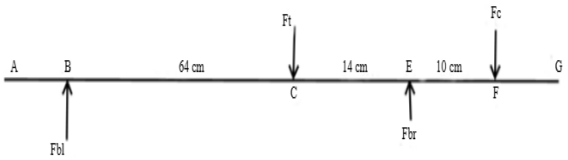

Figure 8 Free body diagram of forces on output shaft at horizontal plane

Using trigonometric relations,

$$Fcx = Fc\cos\gamma, Fbrx = Fbr\cos\emptyset, Fblx = Fbl\cos\emptyset \text{ and } Ft = Fg\cos\varepsilon$$

In order to evaluate horizontal component of bearing reaction forces F_{bl} and F_{br}, was considered bending moment at F:

$$\sum MA = 0 - Fg\cos\varepsilon \times 0.64m + Fbr\cos\emptyset \times 0.78m - Fc\cos\gamma \times 0.88m$$

$$Fg\cos\varepsilon = Ft = 1106.27N$$

$$Fc = T = 821.23N$$

The chain drive was inclined to 20^o to horizontal. Hence,

$Fc\cos\gamma = 821.23N \times \cos 20^o = 771.7N$, then

$$\sum MF = 0$$

$$-1106.27N \times 0.64m + Fbr\cos\emptyset \times 0.78 - 771.7N \times 0.88 = 0$$

$$Fbr\cos\emptyset = 1778.33N$$

Similarly, the horizontal bearing reaction forces F_{bl}, was calculated using total load at E:

$$\sum ME = 0 = Fg\cos\varepsilon - Fbl\cos\emptyset + Fc\cos\gamma - Fbr\cos\emptyset$$

$$1106.27N - Fbl\cos\emptyset + 771.7N - 1778.33N$$

Hence, $Fbl\cos\emptyset = 99.64N$

The horizontal bending moments on the output shaft were:

$$\sum MF = Fg\cos\varepsilon \times 0.24m - Fbr\cos\emptyset \times 0.1m - Fbl\cos\emptyset \times 0.88m$$

$$1106.27N \times 0.24m - 1778.33N \times 0.1m - 99.64N \times 0.88 = 0$$

$$\sum ME = -Fc\cos\gamma \times 0.08m = -77.17Nm$$

$$\sum Mc = Fbr\cos\emptyset \times 0.14m - Fc\cos\emptyset \times 0.24m = 1778.33N \times 0.14m - 771.7N \times 0.24m = 63.75Nm$$

$$\sum MF = -1106.27N \times 0.64m + Fbr\cos\emptyset \times 0.78m - Fc\cos\gamma \times 0.88m - 1106.27N \times 0.64m + 1778.33N \times 0.78m - 771.7N \times 0.88m = 0$$

Based on the magnitude and location of all forces acting on the output shaft, shear force and bending moment on the horizontal plans containing the spur gear and conveyor chain were computed as in figure below.

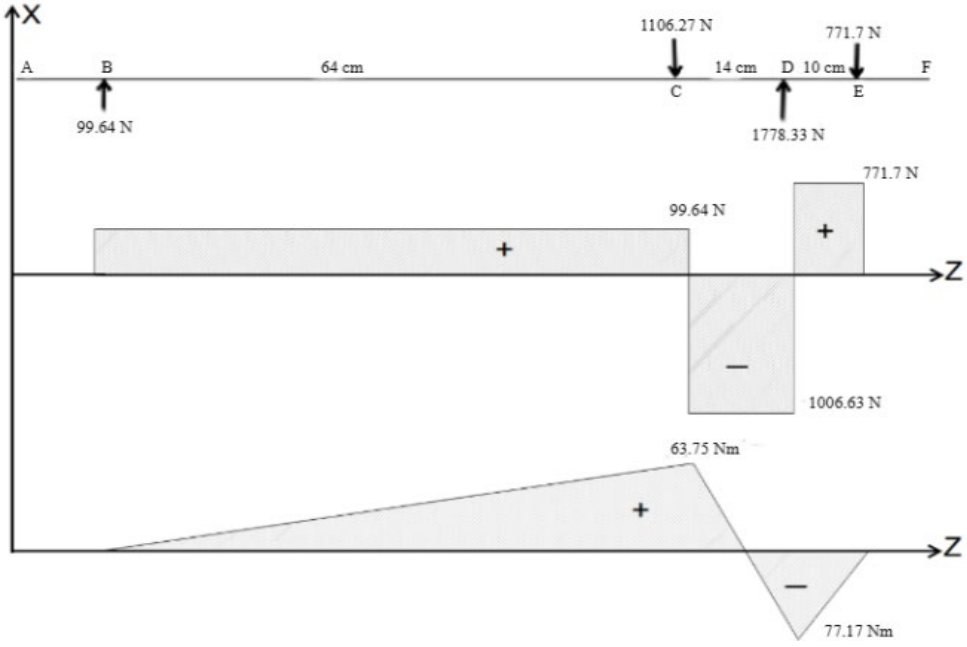

Figure 9 Shear force and bending moment diagrams on vertical directions of the shaft

The diameters of the output shaft were determined using maximum shear stress theory using equation.

From the above bending moment diagram the maximum bending moment and maximum torque

transmitted by output shaft, were 27.54 N m and 63.75 N m at point G, respectively, Assume K_b = 1.5 and K_t = 1, and allowable Stress, 40 MPa (for steel shaft with keyway) was used.

$$do^3 = \frac{16}{\pi\tau}\sqrt{(KbMb)^2 + (KtMt)^2} \quad (41)$$

$$\frac{16}{\pi \times 40Mpa}\sqrt{(1.5 \times 63750Nmm)^2 + (2 \times 2750Nmm)^2}$$

$$21.51mm \approx 25mm$$

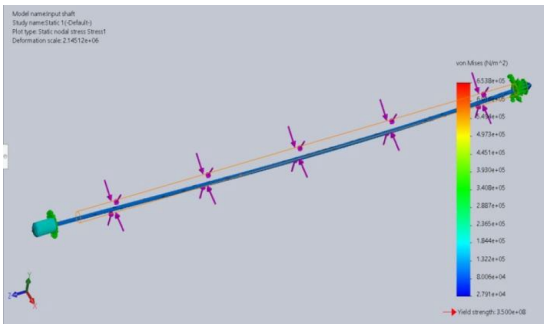

Figure 10 Solid work force analysis on output shaft

Von Mises is a measure of the stress in a material, given in units of Newton's per square meter. In figure shown below, von Mises stress values for different points in a material. The values are given in scientific notation, where "e" represents "times ten to the power of". The values were ranging from $6.538e^{+05}$ to $8.006e^{+04}$ N m^{-2}. These values can be used to analyze the behavior of the material under stress and determine if it is likely to fail or deform

2.9 Design and analysis of input shaft

The input shaft is a cylindrical piece of metal with grooves or "keyways" cut into it that was used to transfer power from the 2WT clutch to other parts in the system. To drive the input shaft, pair of V-belts and pulleys was used to transfer the power from the 2WT clutch. The shaft was then held in place by bearings, with a pulley and driver gear attached that was subject to both twisting and bending forces (as shown in Figure 11).

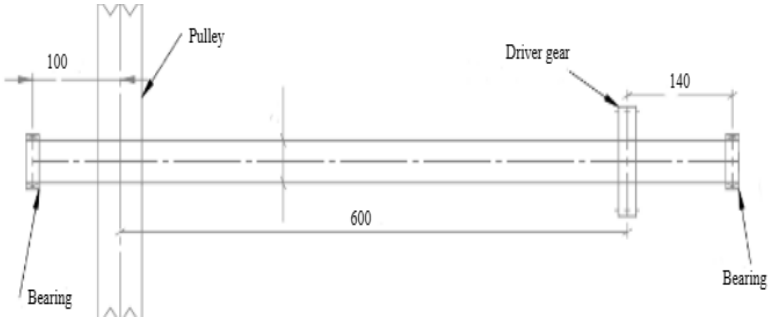

Figure 11 Input shaft profile

Load on input shaft are applied vertical and horizontal directions in xyz plane as shown in Figure 12.

Figure 12 The forces acting on input shaft

Shear force and bending moment diagram on horizontal plane was:

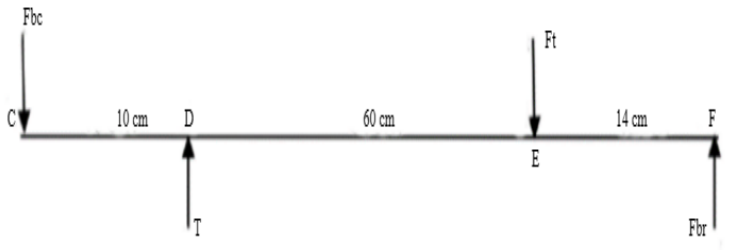

Figure 13 Free body diagram of the input shaft on horizontal plane

Using trigonometric relation:

$$Fbc = Fbc\cos\alpha, \text{and } Fbc = Fbr\cos\theta \quad (42)$$

Gear forces and belt tension was:

$Ft = 1106.27N$, $Fn = 402.65N$ and $T = T1 + T2 = 668.95N$

Determine reaction forces F_{brx} and F_{blx}, through moment at L and O was:

$$\sum Mc = (T1 + T2) \times 0.1m - Ft \times 0.70m + Fbr\cos\theta \times 0.84m = 0 = (668.95N) \times 0.1m - 1106.27N \times 0.70m + Fbr\cos\theta \times 0.84m$$

$$Fbr\cos\theta = 842.25N$$

$$\sum Fx = -T + Ft + Fbc\cos\alpha - Fbr\cos\theta = -668.95N + 1106.27N + Fbc\cos\alpha - 842.25N$$

$$Fbc\cos\theta = 404.93N$$

Then, the horizontal moment of input shaft would be:

$$\sum ME = Fbr\cos\theta \times 0.14m = 842.25N \times 0.14m = 117.91Nm$$

$$\sum MD = -Ft \times 0.60m + Fbr\cos\theta \times 0.74m = -1106.27N \times 0.60m + 842.25N \times 0.74m = -40.5Nm$$

$$\sum Mc = (T1 + T2) \times 0.1m + Fbr\cos\theta \times 0.84m - Ft \times 0.70m = 668.95N \times 0.1m + 842.25N \times 0.84m - 1106.27N \times 0.70m = 0$$

Based on the magnitude and location of forces acting on the input shaft, shear force and bending moment on the horizontal plane of the shaft were computed and plotted as follows:

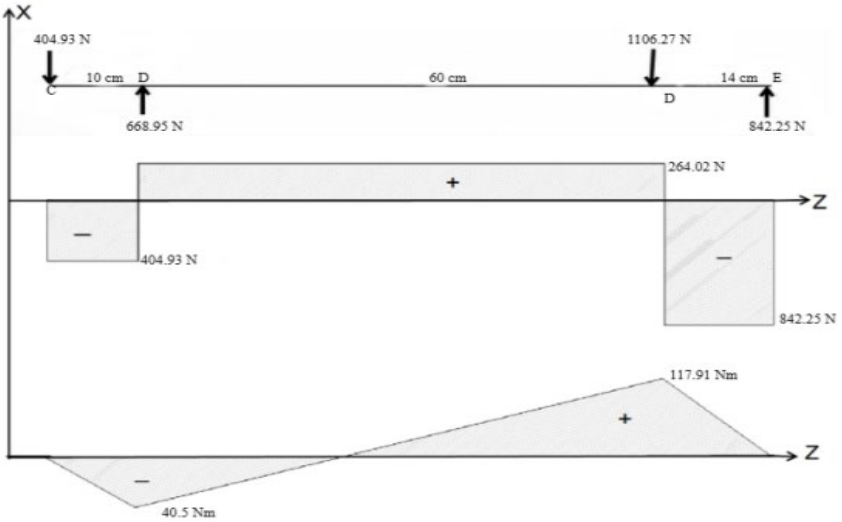

Figure 14 Horizontal plane shear and bending moment diagrams on the shaft

Shear force and bending moment diagram on vertical plane was:

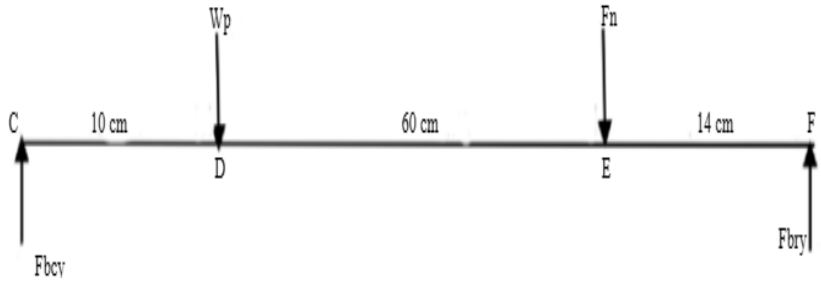

Figure 15 Free body diagram of the input shaft on vertical plane

Using trigonometric relations:

$$Fbc\sin\alpha = Fbcy, \text{and } Fbr\sin\theta = Fbry \quad (43)$$

Assume no slip of gear and belt, the vertical component of bearing reaction force was computed through moments at C and F. respectively:

$$\sum Mc = 0 = Wp \times 0.1m - Fn \times 0.70m + Fbr\sin\theta \times 0.84m = 22.84N \times 0.1m - 402.65N \times 0.70m + Fbr\sin\theta \times 0.84m$$

$$Fbr\sin\theta = 332.82N$$

Equilibrium of vertical forces (F_y):

$$\sum Fy = -Fbclsin\theta + Wp + Fn - Fbrsin\theta = 0 - Fbclsin\theta + 22.84N + 402.65N - 332.82N, \text{then } Fbclsin\theta = 92.67N$$

Total bending moments of input shaft on vertical plane

$$\sum ME = Fbrsin\theta \times 0.14m = 332.82N \times 0.14m = 46.59Nm$$

$$\sum MD = -Fn \times 0.60m + Fbrsin\theta \times 0.74m = -402.65N \times 0.60m + 332.82N \times 0.74m = 4.7Nm$$

$$\sum Mc = Wp \times 0.1m - Fbrsin\theta \times 0.84m + Fn \times 0.70m = 22.84N \times 0.1m + 402.65N \times 0.70m - 332.82N \times 0.84m = 4.57Nm$$

Shear force and bending moment diagram on vertical plane.

The maximum torque on the input shaft (M_t) developed through machine pulley was: T_t =530.45 N and T_s=138.5 N m).

$$Mt = (Tt - Ts)Dp = (530.45N - 138.5N) \times 0.255m = 99.95Nm$$

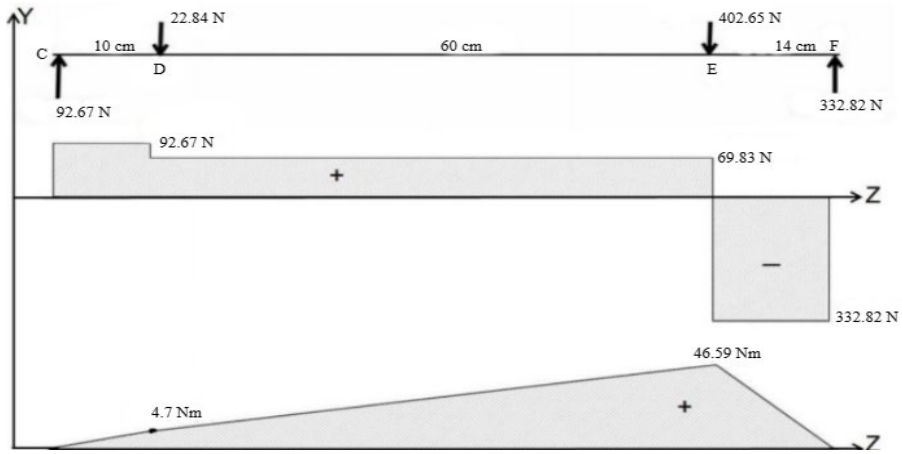

Figure 16 Vertical plane shear and bending moment diagrams on input shaft

Using Equation (41), the diameters of the input shaft were determined as follows:

$$\frac{16}{\pi \times 40Mpa}\sqrt{(1.5 \times 117910\ Nmm)^2 (99950\ Nmm)^2} \approx 30mm$$

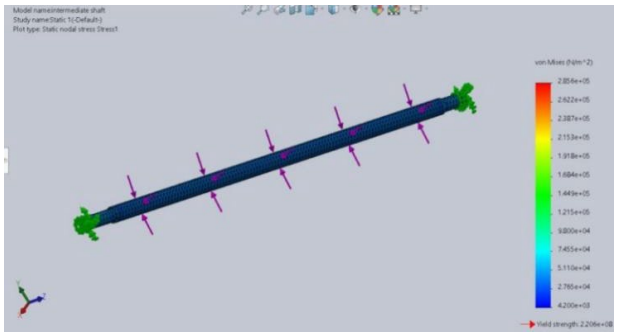

Figure 17 Force analysis on input shaft

A model is a representation of a system or process used to study its behavior or performance. "Input shaft" is the name given to the model being studied. "Static 1" refers to a type of study where the system is analyzed under static conditions, i.e., when it is not in motion. "Static displacement Displacement1" refers to the type of plot being generated, which shows the displacement of the system under static conditions. Deformation scale is a measure of the amount of deformation or distortion in the system being studied. In this case, the deformation scale used is 2:14512e^{+06}.

2.10 Selection of V-belt and pulley

2.10.1 Selection of pulley

The driver pulley and driven pulley are components of a two-wheel tractor's engine and a machine, respectively. The diameter of the clutch, which connects the driver and driven pulley was 21.2 mm. The rpm of the driver pulley/clutch of the tractor and the driven/machine pulley were 48.74 m s^{-1} and 25.18 m s^{-1}, respectively. The diameter of the driven pulley was calculated using Equation 44 based on the necessary rpm.

$$Nc \times Dc = Nm \times Dm \quad (44)$$

$$Dm = \frac{Nc \times Dc}{Nm} = \frac{\frac{48.74m}{s} \times 212mm}{\frac{29.66m}{s}} = 255mm$$

Aluminum pulley with 255 mm diameter was purchased from market.

2.10.2 Selection of V-belt

The V-belt drive transmits power from a motor attached to a clutch to a machine such as a pulley. In this particular case, the net power being transmitted was 11.03 kW at a speed of 42.9 m s^{-1}. The machine was running 8 hours a day, and a correction factor was applied that was equal to 1.2. Hence, design power (Pds) was (Bhandari, 2010):

$$Pds = Ptr \times fa \quad (45)$$

$$Pds = 10.3 \times 1.2 = 12.36\,Kw$$

The selected belt used to drive 12.36 kW design power and 42.9 m s^{-1} was B-section V-belt. Therefore, diameter of driver (d) (clutch) and driven (D) pulley (machine pulley) were 212 mm and 255 mm respectively. Pitch length of belt (Lb) using equation below.

$$Lb = 2C + \frac{\pi(D+d)}{2} + \frac{(D-d)^2}{4C} \quad (46)$$

$$Lb = 2450mm + \frac{\pi(255mm + 212mm)}{2} + \frac{(255mm-212mm)^2}{4C} = 1634.22mm$$

The required pitch length for B section belt was around 1700mm (Using quadratic equation theorem, the corrected center distance was:

$$1700mm = 2 \times C + \frac{\pi(255mm + 212mm}{2} + \frac{(255mm-212mm)^2}{4C}$$

$$2C^2 - 966.81C + 462.25 = 0, C = 483mm$$

Determination of the number of belts required was estimated as follows:

The speed ratio (Sr) was:

$$Sr = \frac{\frac{42.9m}{s}}{\frac{20.95m}{s}} = 1.46$$

2.11 Selection of bearings

The bearing that is best for the machine's nature, the area inside the machine, the spindle specification, the lubrication system, and the drive system must consider the bearing's design life, precision, rigidity, critical speed, and other properties. A square flange and four drill holes for attaching bolts with shaft sizes ranging from 15 to 100 mm are present in the housings. For metric shafts, there are two sets of bearing units depending on the housing design (ASTM, 2014).

2.12 Depth control systems

According to Dessye (2021), the mechanism for depth control system was constructed to set up variation of harvesting depth. The sliding arm with whole machine body slides by rotation of screw to change depth of operation during transport as well as operations. The power screw rotates manually by a handle, which fixed on both side of operator site on side flanges. Acme threaded screw with 28 mm; 13.5 mm and 4 mm outer diameter, inner diameter and pitch diameter respectively were selected. Angle of acme threads (2β), where, β = 14.5° (Bansal, 2009). The screw with single start acme threads of 28mm nominal diameter and 5mm pitch is suitable for depth control system of the machine (Dessye, 2021). The depth of the lift arm varied within a range of zero to 150 mm vertically as shown Figure 18:

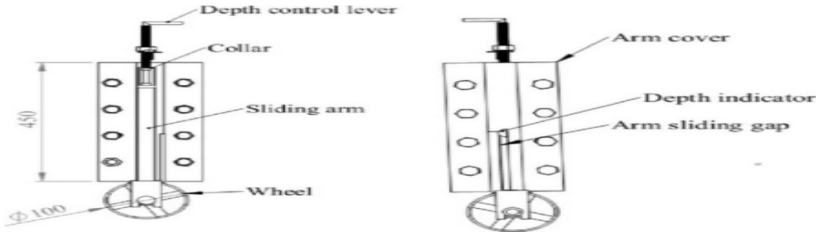

Figure 18 Depth control system

2.13 Cutting disc

Cutting disc has the diameter of 333 mm and 6 mm thickness was sharpened using grinder for easily slicing the soil.

2.14 Performance evaluation of onion harvester

Onion was planted on both raised and flat beds in Kulumsa agricultural research center. Planting of onion was done with a manual row planting. The onion

crop was ready for harvesting after 120 days of planting. Harvesting was carried out in the month of January 2024.

2.14.1 Percentage of damaged onion bulbs

Damage occurs during digging, loading, and transporting operations. The damage resulting of impact on bulbs during harvesting operations alone may cause losses in excess of 20% (Storey and Davies, 1992). Damage to bulb within permissible limit was less than 5 per cent (Basavaraj and Jayan, 2020). Percentage of damage was determined on 2m length of row randomly marked and collected and counted all the visible bulbs through collector of onion digger and surface. The damaged bulbs were separated and counted and undamaged onion bulbs after harvesting and recorded as percentage of damage. The damage percentage could be calculated using equation below (Ibrahim et al., 2008).

$$\eta d = \frac{Md}{Mnd + Md} \times 100 \quad (47)$$

Where:

Md = Mass of seriously damaged or cut root crop, kg

M_{nd} = Mass of root crop exposed and not damaged, kg.

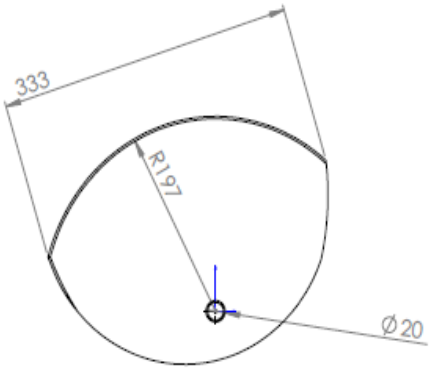

Figure 19 Cutting disc drawing

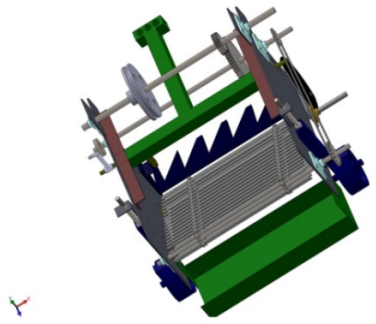

Figure 20 Solid work design of onion harvester

Figure 21 The fabricated onion harvester

2.14.2 Fuel consumption

Before and after the digging operation, the fuel tank of the 2WT was filled to the neck with fuel. The fuel consumption for digging operations was assessed after the test and was expressed as L hr^{-1}. The fuel used to refill the vehicle was measured in milliliters. According to Macmillan (2002) fuel consumption was:

$$Fc = \frac{Cr}{A} \times C1 \quad (48)$$

Where:

F_c = fuel consumption rate, l ha^{-1}

C_r = reading of cylinder, l.

A = area, m^2

C_1 = conversion factor

2.14.3 Wheel slip (S %)

The wheel slip of the tractor with load and without load was measured at 15 m distance. Wheel slip can be calculating by counting the number of revolutions in a given distance (In terms of distances for a given number of wheel revolutions) and recorded as $S_{\%}$ in %Wheel slip can be calculating by counting the number of revolution in a given distance and expressed as (Macmillan, 2002):

$$S = \frac{mo - m}{mo} \times 100 \quad (49)$$

$$mo = 2\pi rNw \quad (50)$$

Where:

N_w = number of wheel revolution, rpm;

r = radius of wheel, m;

m = travel distance measured (length of test truck), m.

2.14.4 Field capacity

Field capacity was an actual field capacity

computed by the actual average time consumed during digging operation (lost time + productive time) and recorded in ha h^{-1} Effective field capacity of the machine is calculating as given below (Zaied et al., 2014).

$$Efc = \frac{A}{Tp + T1} \quad (51)$$

Where:

Efc = Effective field capacity, ha h^{-1};

A = Area covered, ha;

T_p = Productive time, h;

T_l = Non-productive time, h.

2.14.5 Field efficiency

Field efficiency can estimated as (Zaied et al., 2014)

$$Fe = \frac{Efc}{Ct} \times 100 \quad (52)$$

Where:

Fe = Field efficiency, %

Efc = Effective field capacity, ha h^{-1}

C_t = Theoretical field capacity, ha h^{-1}

S = Speed of operation, km/h

2.14.6 Drawbar pulls

The draft requirement of a given machine can be measured using drawbar dynamometer attached to the machine and the power sources or using two tractors and a dynamometer between them. The first tractor was power sources while the second one, which was towed and served as machine/digger carrier. Drawbar pull requirement (Df), a machine was measured using drawbar dynamometer using two tractors and a dynamometer between them; the first tractor was power sources while the second one was towed served as machine/digger attached to it and recorded as D_f in kN.

2.14.7 Missing percentage

The missed onion bulb is harvested by hand and its percentage was calculated according to the data obtained from experimental field.

2.14.8 Digging efficiency

Digging efficiency was calculated using the following equation:

$$\text{Digging efficiency} = \frac{A}{A+B} \times 100 \quad (53)$$

Where:

A = mass of tuber dugout by harvester in unit area, kg;

B = mass of tuber left in soil after harvesting in unit area, kg.

To ensure clarity and accuracy in your study, it's essential to indicate the tested treatments and the statistical design used. Here's a detailed explanation:

(1) Tested treatments: Clearly define the different treatments or conditions that were tested in your study. This could include variations in soil moisture content, harvester speed, tuber variety, or any other relevant factors.

(2) Statistical design: Specify the statistical design used to analyze the data. Common designs include:

For the digging efficiency equation:

Digging efficiency=AA+B×100%

Where:

AA is the mass of tuber dugout by the harvester in a unit area (kg).

BB is the mass of tuber left in the soil after harvesting in a unit area (kg).

This equation helps in determining the efficiency of the harvesting process by comparing the amount of successfully harvested tubers to the total amount of tubers, including those that were not harvested or were damaged

3 Results and discussion

3.1 Onion bulbs damage

Table 1 shows that at the forward speed of 1.39 km h^{-1} the bulb damage was highest at a digging depth of 5cm (4.15%), followed by 7cm (2.48%) and 10cm (1.13%). At a forward speed of 2.47 km h^{-1} the bulb damage was highest at a digging depth of 5 cm (4.46%), followed by 7 cm (2.57%) and 10 cm (1.25%). At a forward speed of 4.15 km h^{-1}, the tuber damage was highest at a depth of operation of 5 cm (4.56%), followed by 7 cm (2.64%) and 10 cm (1.54%). This implies that as depth of operation increases mean onion tuber damage decrease while as forward speed increases; mean onion tuber damage percentage also increases. Generally, maximum value of damage

percentage of onion tuber was 4.56% at forward speed of 4.15 km h^{-1} and digging depth of 5 cm, while the minimum value was 1.13% at forward speed of 1.39 km h^{-1} and digging depth of 10 cm.

3.2 Digging efficiency

The digging efficiency is related with the raised damaged and undamaged onion tubers. At a forward speed of 1.39 km h^{-1} and a depth of operation of 10cm, the harvester had the highest digging efficiency of 97.03%, while at a forward speed of 4.15 km h^{-1} and a depth of operation of 5cm, the harvester had the lowest digging efficiency of 84.60%. Generally, digging efficiency was decreased by increasing the speed from 1.39 – 4.15 km h^{-1}, but the digging efficiency was increased with increasing the digging depth of operation from 5 cm-10 cm.

Table 1 Means with SE of damage percentage at various Fs and digging depth

Treatments	Digging depth (cm)		
F_s(km h^{-1})	5	7	10
1.39	$4.15^{a} \pm 0.52$	$2.48^{b} \pm 0.17$	$1.13^{c} \pm 0.10$
2.47	$4.46^{a} \pm 0.38$	$2.57^{b} \pm 0.22$	$1.25^{c} \pm 0.18$
4.15	$4.56^{a} \pm 0.42$	$2.64^{b} \pm 0.23$	$1.54^{c} \pm 0.36$

Note: Means followed by the same letter's superscript are not significantly different at 5% level of probability; SE = Standard Errors.

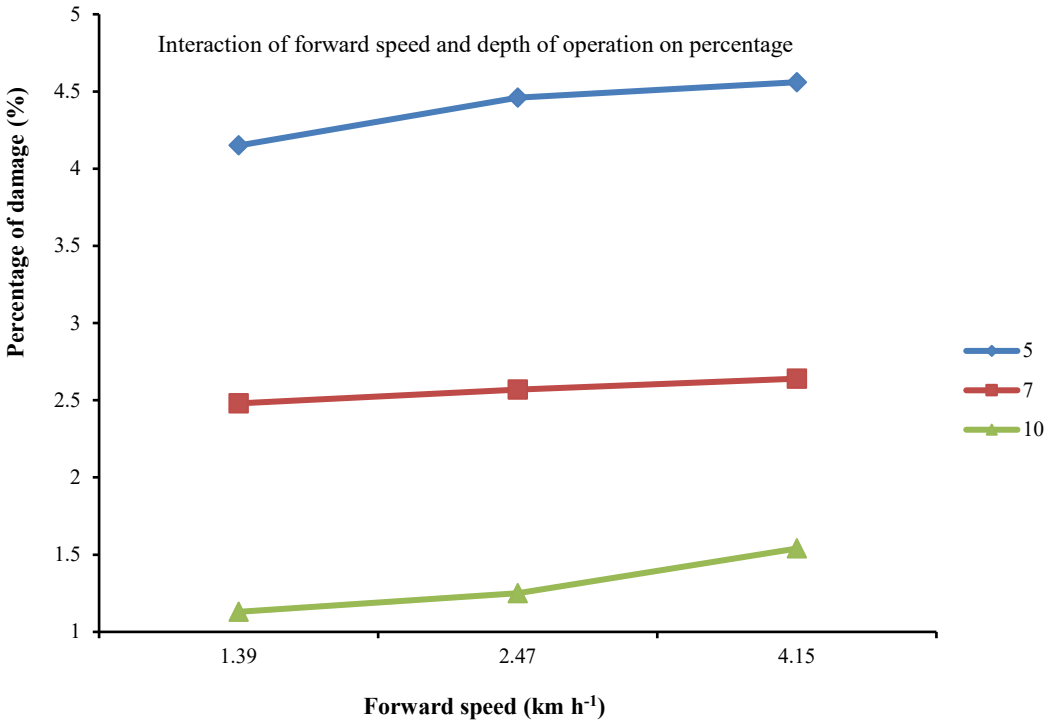

Figure 20 Effect of forward speed and depth of operation on damage percentage

Table 2 Means with SE of digging efficiency at various forward speed and digging depth

Treatments	Digging depth (cm)		
Fs (km h^{-1})	5	7	10
1.39	$87.04^{e} \pm 0.62$	$95.52^{bc} \pm 1.03$	$97.03^{a} \pm 1.06$
2.47	$86.17^{e} \pm 0.37$	$95.40^{c} \pm 0.62$	$96.63^{ab} \pm 0.91$
4.15	$84.60^{f} \pm 0.61$	$93.67^{d} \pm 0.77$	$95.64^{bc} \pm 0.63$

Note: Means followed by the same letter's superscript are not significantly different at 5% level of probability; SE = Standard errors.

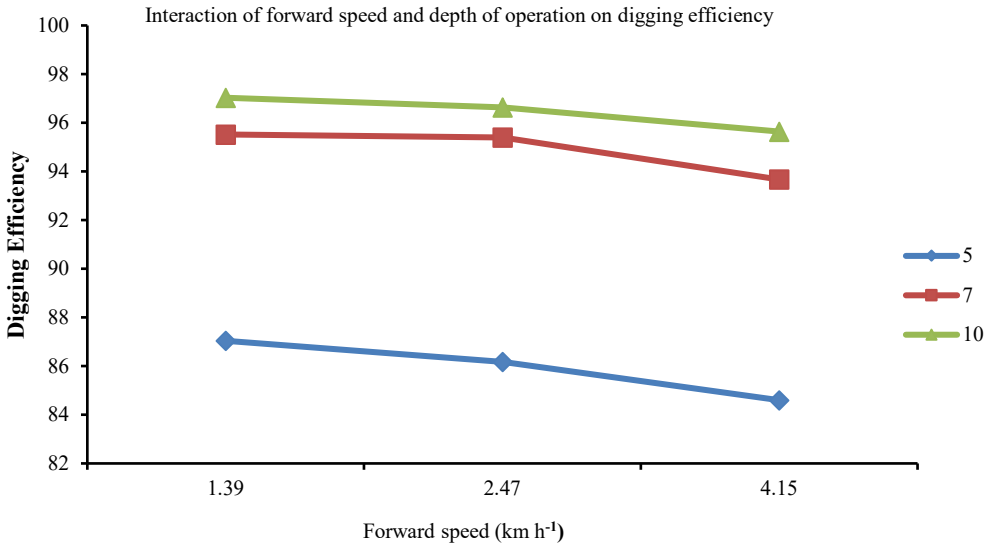

Figure 21 Digging efficiency

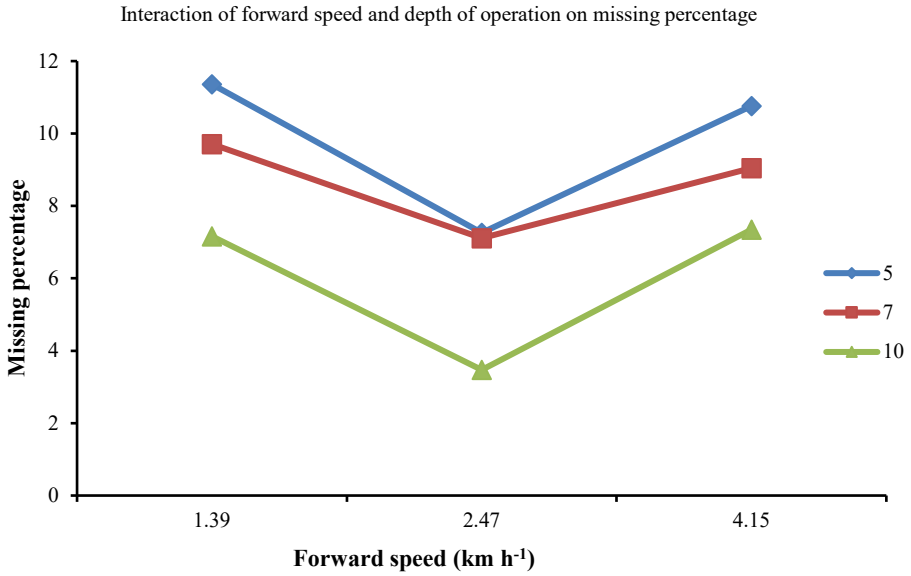

Figure 22 Missing percentage of missing percentage

Table 3 Means with SE of missing percentage at various forward speed and depth of operation

Treatments	Depth of operation (cm)		
Fs (km h^{-1})	5	7	10
1.39	11.36^{a} ± 0.17	9.707^{ab} ± 0.29	7.157^{b} ± 0.31
2.47	7.257^{b} ± 0.35	7.11^{b}± 0.24	3.470^{c}± 0.14
4.15	10.76^{a} ± 0.12	9.047^{ab} ± 0.04	7.347^{b} ± 0.05

Note: Means followed by the same letter's superscript are not significantly different at 5% level of probability; SE = Standard errors.

3.3 Missing percentage

Table 3 shows that the means and standard errors (SE) of missing percentage of onion digger at various forward speeds and depths of operation. The percentage of missing tubers decreased with increasing the speed from 1.39 km h^{-1} to 2.47 km h^{-1}. After increasing speed from 2.47 to 4.15 km h^{-1}, the missing tubers percent increased due to increasing the slip. It was noticed that with increasing the digging depth, the missing tubers decreased due to the distance between the top of the line and the lowest point of the tubers range from 5 to 10 cm. The maximum value of missing tubers was 11.36% at forward speed of 1.39 km h^{-1} and digging depth of 5 cm, while the minimum value was

3.47% at forward speed of 2.47 km h^{-1} and digging depth of 10 cm.

3.4 Drawbar pull

Table 4 shows that the means with standard errors (SE) of the onion digger at various forward speeds and depths of operation. The table also shows that the highest mean value of the onion digger was observed at 4.15 km hr^{-1} forward speed and 10 cm depth of operation, which was 2935.4 N. The lowest mean value was observed at 1.39 km h^{-1} forward speed and 5 cm depth of operation, which was 2772.4 N. The results imply that draft increased with increase of depth of operation and forward speed.

3.5 Fuel consumption

Table 5 shows that the mean values of fuel consumption (Fc) for the onion digger at different forward speeds and depths of operation. Maximum fuel consumption was 15.51 L ha^{-1} at 4.15 km h^{-1} forward speed and 10cm depth of operation and minimum fuel consumption was 12.36 L ha^{-1} at 1.39 km h^{-1} and 5 cm depth of operation. For summarizing, fuel consumption of the machine increased with in increasing both forward speed and depth of operation.

Table 4 Means with SE of DF (N) at various forward speeds and depths of operation

Treatments	Depth of operation (cm)		
Fs (km h^{-1})	5	7	10
1.39	$2772.4^{g} \pm 22.45$	$2824.7^{d} \pm 40.09$	$2904.5^{a} \pm 88.57$
2.47	$2779.9^{h} \pm 23.16$	$2835.0^{e} \pm 32.51$	$2921.1^{b} \pm 81.08$
4.15	$2786.9^{i} \pm 22.57$	$2846.2^{f} \pm 35.16$	$2935.4^{c} \pm 78.18$

Note: Means followed by the same letter's superscript are not significantly different at 5% level of probability; SE = Standard Errors.

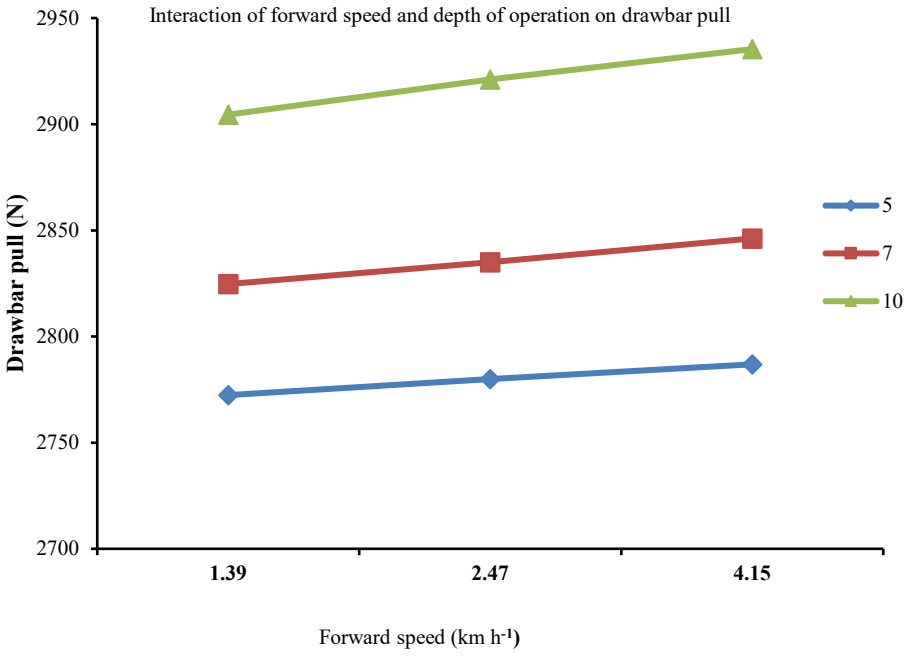

Figure 23 Drawbar pull

Table 5 Means with SE of fuel consumption (Fc) at various forward speed and depth of operation

Treatments	Digging depth (cm)		
Fs (km h^{-1})	5	7	10
1.39	$12.36^{e} \pm 0.13$	$12.56^{de} \pm 0.31$	$12.73^{cde} \pm 0.33$
2.47	$13.05^{cde} \pm 0.60$	$13.65^{bcd} \pm 0.78$	$13.85^{bc} \pm 0.16$
4.15	$14.54^{ab} \pm 0.40$	$15.12^{a} \pm 0.36$	$15.51^{a} \pm 0.50$

Note: Means followed by the same letter's superscript are not significantly different at 5% level of probability; SE = Standard Errors.

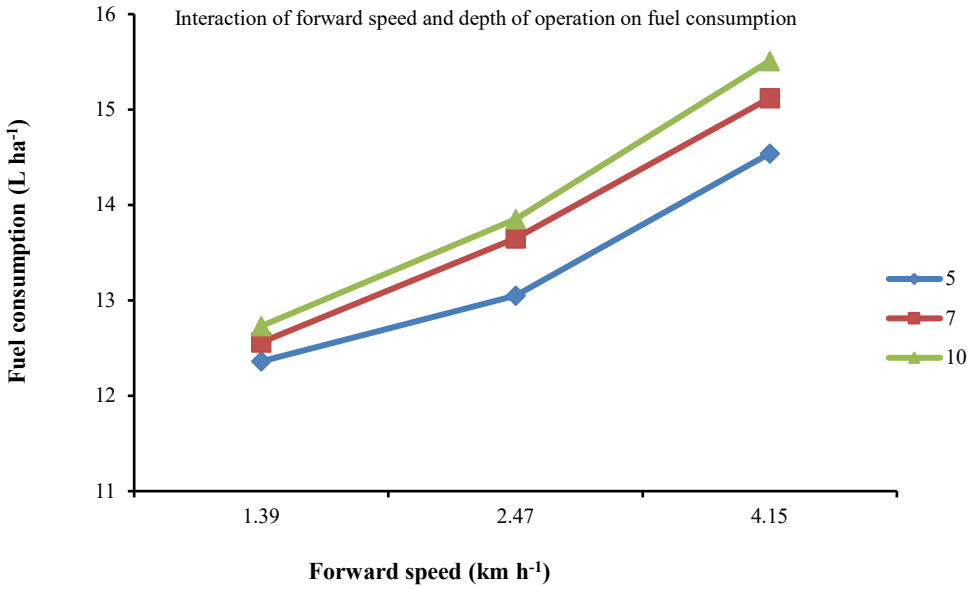

Figure 24 Fuel consumption

Table 6 Means with SE of field capacity (Fca) at various forward speed and depth of operation

Treatments	Depth of operation (cm)		
Fs (km h^{-1})	5	7	10
1.39	0.147^{a} ± 0.0068	0.140^{a} ± 0.0025	0.135^{a} ± 0.0021
2.47	0.155^{a} ± 0.0032	0.146^{a} ± 0.0035	0.139^{a}± 0.0055
4.15	0.157^{a} ± 0.0038	0.151^{a} ± 0.0011	0.143^{a} ± 0.0064

Note: Means followed by the same letter's superscript are not significantly different at 5% level of probability; SE = Standard Errors.

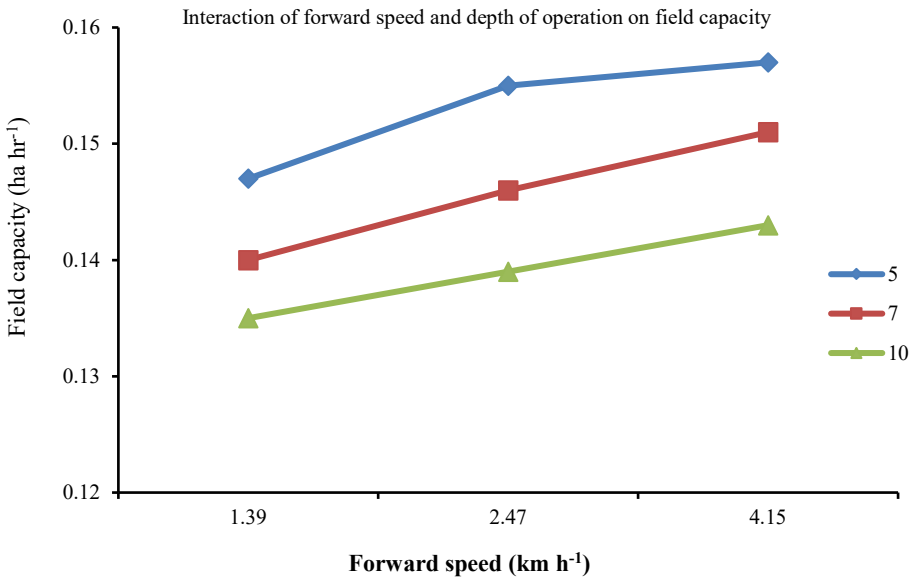

Figure 25 Field capacity

3.6 Field capacity

Table 6 shows that the means with standard errors (SE) of field capacity (Fca) of an onion digger at various forward speeds (Fs) and depths of operation. The field capacity was affected directly by forward speed and depth of operation. The digger field capacity was increased by increasing the forward speed from 1.39 to 4.15 km h^{-1} and decreased by increasing the digging depth from 5cm to 10cm due to increased force with increasing the depth. The maximum value of the digger field capacity was 0.157 ha h^{-1} at forward speed of 4.15 km h^{-1} and digging depth of 5 cm, while the

minimum value was 0.135 ha h^{-1} at forward speed of 1.39 km h^{-1} and digging depth of 10 cm

3.7 Field efficiency

Table 7 shows that the means with standard errors (SE) of field efficiency of an onion digger at various forward speeds and depths of operation. Increasing forward speed from 1.39 to 4.15 km h^{-1} decreased field efficiency and increasing the depth of harvest from 5 to 10 cm decreases field efficiency. Mean maximum field efficiency was 90.84 at minimum forward speed of 1.39 km h^{-1} and at minimum digging depth of 5 cm. Mean minimum field efficiency was 73.06 at maximum forward speed of 4.15 km h^{-1} and at maximum digging depth of 10 cm. In general, field efficiency of the machine decreased with in increasing both forward speed and digging depth. The major reason for the reduction in field efficiency by increasing forward speed may be due to the increasing maintenance requirement by increasing depth and increasing the quantity of soil on the elevator device.

Table 7 Means with SE of Field efficiency of onion digger at various forward speeds and depth of operation

Treatments	Depth of operation (cm)		
Fs (km h^{-1})	5	7	10
1.39	$90.84^{a} \pm 0.17$	$82.18^{c} \pm 0.29$	$78.37^{d} \pm 0.31$
2.47	$85.77^{b} \pm 0.35$	$78.81^{d} \pm 0.24$	$76.26^{e} \pm 0.14$
4.15	$82.33^{c} \pm 0.12$	$76.75^{e} \pm 0.04$	$73.06^{f} \pm 0.05$

Note: Means followed by the same letter's superscript are not significantly different at 5% level of probability; SE = Standard Errors.

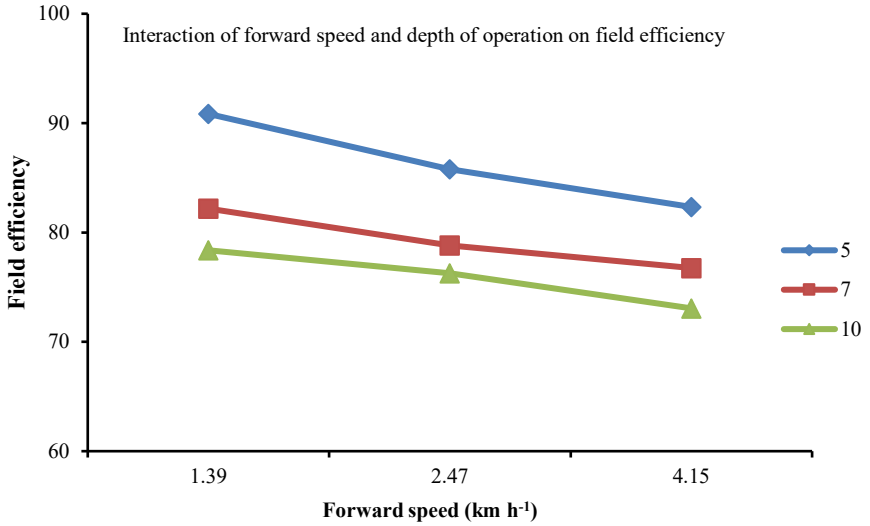

Figure 26 Field efficiency

Table 8 Means with SE of wheel slip of onion digger at various forward speeds and depth of operation

Treatments	Depth of operation (cm)		
Fs (km h^{-1})	5	7	10
1.39	$4.47^{f} \pm 0.78$	$7.33^{e} \pm 0.85$	$9.53^{d} \pm 0.33$
2.47	$8.01^{e} \pm 0.62$	$12.31^{c} \pm 0.43$	$15.22^{b} \pm 0.59$
4.15	$10.5^{d} \pm 0.63$	$15.28^{b} \pm 0.70$	$20.82^{a} \pm 1.72$

Note: Means followed by the same letter's superscript are not significantly different at 5% level of probability; SE = Standard Errors.

3.8 Wheel slip

Table 8 shows that the means with standard errors (SE) of wheel slip of an onion digger at various forward speeds and depths of operation. Mean maximum wheel slip was 20.82% at maximum forward speed of 4.15 km h^{-1} and maximum depth of operation at 10 cm. While, mean minimum wheel slip was 4.47% at minimum forward speed of 1.39 km h^{-1} and minimum depth of operation at 5cm. In general, wheel slip of the machine increased with increasing both forward speed and digging depth.

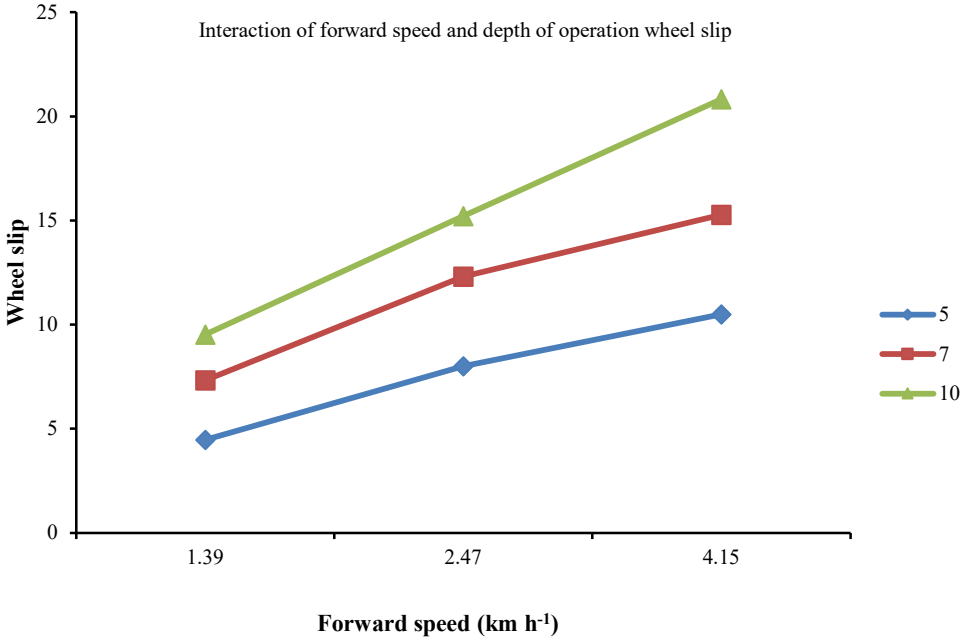

Figure 27 Wheel slip

4 Conclusion

When designing a two-wheel tractor-operated onion harvester, it is essential to consider how forward speed and digging depth affect key performance metrics like fuel efficiency, draft requirement, crop handling, and field capacity. Higher forward speeds improve field capacity but can increase fuel consumption if the engine is under strain. Optimal speed should balance speed with fuel economy. Digging depth correlates with draft greater depths require higher pulling force, which can strain the tractor and compromise efficiency. A slower forward speed and an appropriate digging depth help minimize crop loss and ensure thorough harvesting. Excessive speed might leave onions unharvested or damaged. Forward speed and draft force impact wheel slip, which should be minimized to maintain traction and avoid energy loss. Adequate weight distribution and tire configuration can help reduce slip. Higher forward speeds increase operational efficiency by covering larger areas, but must align with the ability to maintain proper digging depth and minimal crop loss. In conclusion, the design parameters should aim to achieve an equilibrium between forward speed and digging depth to optimize overall performance.

References

Aklilu, S. 1994. Onion research and production in Ethiopia. Acta Horticulturae, 433: 95–98.

American Society for Testing and Materials. 2002. ASTM D3080/D3080M-11. Standard test method for shear strength of soil by direct shear test. West Conshohocken, PA, USA: ASTM International.

American Society for Testing and Materials. 2014. ASTM A29/A29M. Standard specification for the design of shafts. West Conshohocken, PA, USA: ASTM International.

Anon. 2008. Agricultural mechanization and energy management. In *Annual report of Indian Council of Agricultural Research*, 81-85. New Delhi, India.

Bansal, R. K. 2009. *A textbook of strength of materials. 8th ed.* Laxmi Publications. pp. 234–235.

Basavaraj, and P. R. Jayan. 2020. Biometric and engineering properties of ginger rhizome towards the development of root crop harvester. *International Journal of Chemical Studies*, 8(3): 725–730.

Bhandari, V. B. 2010. *Design of Machine Elements*. 3rd ed. New Delhi, India: McGraw-Hill Global Education Holdings LLC.

Bernacki, H., J. Haman, and C. Kanafojski. 1972. Agricultural machines: Theory and Construction. Washington, DC, USA: U.S. Department of Agriculture and the National Science Foundation.

Brewster, J. L. 2008. Onions and Other Vegetable Alliums. Wallingford: CABI.

Budhale, K. C., A. G. Patil, V. S. Shirole, S. S. Patil, R. S. Desai, and S. B. Salavi. 2019. Design and development of digging and conveyor system for self-propelled onion harvester. *International Research Journal of Engineering and Technology*, 6(4): 3304–3307.

Fikre, D. 2021. Regional onion production analysis in Ethiopia. *Journal of Agricultural Studies*, 6(3): 45-60

Dessye, B. 2021. Design, construction and performance evaluation of potato harvester. Ethiopian Institute of Agricultural Research, Agricultural Engineering Research, Fogera National Rice Research and Training Center, 8: Article 2395-0072.

Elyazaji, A. 2024. Global onion production trends. *Journal of Agricultural Economics*, 55(1):123-140.

Erokhin, M. N., A. S. Dorokhov, A. V. Sibirev, A. G. Aksenov, M. A. Mosyakov, N. V. Sazonov, and M. M. Godyaeva. 2022. Development and modeling of an onion harvester with an automated separation system. *AgriEngineering*, 4(2): 380–399.

Etana, M. B., M. C. Aga, and B. O. Fufa. 2019. Major onion (Allium cepa L.) production challenges in Ethiopia: A review. *Journal of Biology, Agriculture and Healthcare*, 9(7): 42-47.

Hatem, A., Smith, J., & Brown, L. 2014. Effects of storage conditions on the hardness of onion bulbs. *Journal of Agricultural Science*, 12(3), 45-58.

Hettiaratchi, D. R. P., B. D. Witney, and A. R. Reece. 1966. The calculation of passive pressure in two-dimensional soil failures. *Journal of Agricultural Engineering Research*, 11(2): 89–107.

Hunde, N. F. 2017. Opportunity, problems and production status of vegetables in Ethiopia: A review. *Journal of Plant Science Research*, 4(2): 172.

Ibrahim, A., Smith, J., & Khan, R. 2008. Assessment of damage percentage in agricultural produce. *International Journal of Agricultural Sciences*, 15(2), 123-130.

Kebede, L., and B. Getnet. 2017. Performance of single axle tractors in the semi-arid central part of Ethiopia. *Ethiopian Journal of Agricultural Sciences*, 27(1): 37–53.

FAOSTAT. 2019. Food and Agriculture Organization Statistical Division Retrieved from http://www.fao.org/faostat/en/?#data/QC.

Khura, T. K. 2008. Design and development of tractor drawn onion digger. Ph.D. diss., Indian Agricultural Research Institute, New Delhi, India.

Khurmi, R. S., & Gupta, J. K. 2005. *Theory of machines*. 5th ed. New Delhi, India: Eurasia Publishing House.

Kitila, C., A. Abraham, and S. Shuma. 2022. Growth and bulb yield of some onion (Allium cepa L.) varieties as influenced by NPS fertilizer at Dambi Dollo University research site, Western Ethiopia. *Cogent Food & Agriculture*, 8(1): 2097606.

Laryushin, N. P., and A. M. Laryushin. 2009. Energy-saving onion harvesting technology. *Russian Agricultural Sciences*, 35(1): 66–67.

Macmillan, R. H. 2002. The Mechanics of Tractor–implement Performance: Theory and Worked Examples. Melbourne, Australia: The University of Melbourne.

McKyes, E. 1989. Exploration of Soil Mechanics Principles and Their Applications in Agricultural Engineering. Montréal, Quebec, Canada: Elsevier Science Publishers B.V.

Mohsenin, N. N. 1986. Physical Properties of Plant and Animal Materials. 2nd ed. New York, USA: Gordon and Breach Science Publishers.

Mott, R. L. 2004. *Machine Elements in Mechanical Design*. 4th ed. New Jersey, USA: Pearson Prentice Hall.

Sharma, D. N., & Mukesha, S. 2010. *Farm machinery principles and problems.* 2nd ed. New Delhi, India: Jain Brothers.

Storey, M., & Davies, H. V. 1992. Tuber quality and storage. In *The Potato Crop: The Scientific Basis for Improvement*, ed. P. M. Harris, 507–569. London, UK: Springer

Zaied, M. B., A. M. El Naim, M. H. Dahab, and A. S. Mahgoub. 2014. Development of powered groundnut harvester for small and medium holdings in North Kordofan state in Western Sudan. *World Journal of Agricultural Research*, 2(3): 119–123.